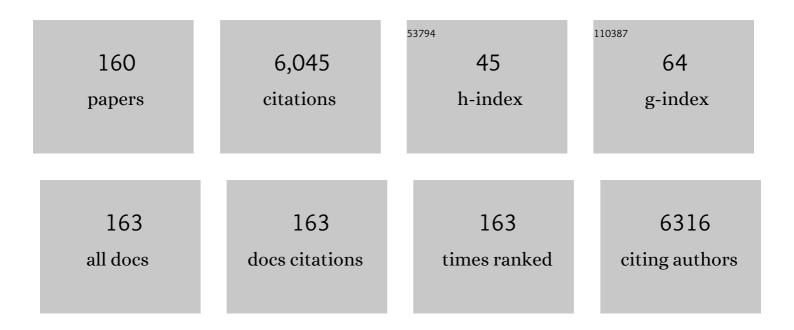
List of Publications by Year in descending order

Source: https://exaly.com/author-pdf/1943230/publications.pdf Version: 2024-02-01



#	Article	IF	CITATIONS
1	Robust superhydrophobic attapulgite coated polyurethane sponge for efficient immiscible oil/water mixture and emulsion separation. Journal of Materials Chemistry A, 2016, 4, 15546-15553.	10.3	317
2	N-doped mesoporous FeNx/carbon as ORR and OER bifunctional electrocatalyst for rechargeable zinc-air batteries. Electrochimica Acta, 2019, 296, 653-661.	5.2	135
3	Core-shell structured Ni3S2@Co(OH)2 nano-wires grown on Ni foam as binder-free electrode for asymmetric supercapacitors. Chemical Engineering Journal, 2018, 345, 48-57.	12.7	122
4	Facile synthesis of carbon-supported pseudo-core@shell PdCu@Pt nanoparticles for direct methanol fuel cells. International Journal of Hydrogen Energy, 2011, 36, 839-848.	7.1	119
5	Mesoporous nickel-sulfide/nickel/N-doped carbon as HER and OER bifunctional electrocatalyst for water electrolysis. International Journal of Hydrogen Energy, 2019, 44, 2832-2840.	7.1	112
6	Rational Design of Hierarchically Core–Shell Structured Ni <sub>3</sub> S <sub>2</sub> @NiMoO <sub>4</sub> Nanowires for Electrochemical Energy Storage. Small, 2018, 14, e1800791.	10.0	111
7	Control of MnO2 nanocrystal shape from tremella to nanobelt for ehancement of the oxygen reduction reaction activity. Journal of Power Sources, 2015, 280, 526-532.	7.8	107
8	CoNiSe2 nanorods directly grown on Ni foam as advanced cathodes for asymmetric supercapacitors. Chemical Engineering Journal, 2019, 364, 320-327.	12.7	104
9	Rich-grain-boundary of Ni <sub>3</sub> Se <sub>2</sub> nanowire arrays as multifunctional electrode for electrochemical energy storage and conversion applications. Journal of Materials Chemistry A, 2019, 7, 3344-3352.	10.3	97
10	Engineered porous Ni2P-nanoparticle/Ni2P-nanosheet arrays via the Kirkendall effect and Ostwald ripening towards efficient overall water splitting. Nano Research, 2020, 13, 2098-2105.	10.4	92
11	Nitrogen-rich mesoporous carbon derived from melamine with high electrocatalytic performance for oxygen reduction reaction. Journal of Power Sources, 2014, 261, 238-244.	7.8	87
12	Ni(OH) <sub>2</sub> Nanoflakes Supported on 3D Ni <sub>3</sub> Se <sub>2</sub> Nanowire Array as Highly Efficient Electrodes for Asymmetric Supercapacitor and Ni/MH Battery. Small, 2019, 15, e1802861.	10.0	84
13	Strain Effect of Core-Shell Co@Pt/C Nanoparticle Catalyst with Enhanced Electrocatalytic Activity for Methanol Oxidation. Journal of the Electrochemical Society, 2012, 159, B270-B276.	2.9	79
14	The enhanced electrocatalytic activity of okara-derived N-doped mesoporous carbon for oxygen reduction reaction. Journal of Power Sources, 2015, 274, 741-747.	7.8	77
15	Biomass-derived activated carbon as high-performance non-precious electrocatalyst for oxygen reduction. RSC Advances, 2013, 3, 12039.	3.6	76
16	Double-shelled tremella-like NiO@Co3O4@MnO2 as a high-performance cathode material for alkaline supercapacitors. Journal of Power Sources, 2017, 343, 76-82.	7.8	74
17	Core–Shell-Structured Low-Platinum Electrocatalysts for Fuel Cell Applications. Electrochemical Energy Reviews, 2018, 1, 324-387.	25.5	72
18	Mesoporous nickel selenide N-doped carbon as a robust electrocatalyst for overall water splitting. Electrochimica Acta, 2019, 300, 93-101.	5.2	70

#	Article	IF	CITATIONS
19	Facile loading of cobalt oxide on bismuth vanadate: Proved construction of p-n junction for efficient photoelectrochemical water oxidation. Journal of Colloid and Interface Science, 2020, 570, 89-98.	9.4	70
20	Pig bones derived N-doped carbon with multi-level pores as electrocatalyst for oxygen reduction. Journal of Power Sources, 2015, 297, 295-301.	7.8	69
21	Liquid–liquid interface-mediated room-temperature synthesis of amorphous NiCo pompoms from ultrathin nanosheets with high catalytic activity for hydrazine oxidation. Chemical Communications, 2015, 51, 3570-3573.	4.1	64
22	Evolution of nanoscale amorphous, crystalline and phase-segregated PtNiP nanoparticles and their electrocatalytic effect on methanol oxidation reaction. Physical Chemistry Chemical Physics, 2014, 16, 3593.	2.8	61
23	Highly active Vulcan carbon composite for oxygen reduction reaction in alkaline medium. Electrochimica Acta, 2014, 133, 391-398.	5.2	59
24	Highly Efficient Photocatalytic Hydrogen Production of Flower-like Cadmium Sulfide Decorated by Histidine. Scientific Reports, 2015, 5, 13593.	3.3	59
25	N-Doped 3D Porous Ni/C Bifunctional Electrocatalysts for Alkaline Water Electrolysis. ACS Sustainable Chemistry and Engineering, 2019, 7, 3974-3981.	6.7	59
26	Cage-like MnO 2 -Mn 2 O 3 hollow spheres with high specific capacitance and high rate capability as supercapacitor material. Electrochimica Acta, 2016, 219, 540-546.	5.2	58
27	Carbon supported Pt-shell modified PdCo-core with electrocatalyst for methanol oxidation. International Journal of Hydrogen Energy, 2010, 35, 10081-10086.	7.1	57
28	A cost effective, highly porous, manganese oxide/carbon supercapacitor material with high rate capability. Journal of Materials Chemistry A, 2016, 4, 5390-5394.	10.3	56
29	Controlled synthesis of nanostructured Co film catalysts with high performance for hydrogen generation from sodium borohydride solution. Journal of Power Sources, 2013, 239, 277-283.	7.8	55
30	Ranunculus flower-like Ni(OH) <sub>2</sub> @Mn <sub>2</sub> O <sub>3</sub> as a high specific capacitance cathode material for alkaline supercapacitors. Journal of Materials Chemistry A, 2016, 4, 7591-7595.	10.3	55
31	Synergy among manganese, nitrogen and carbon to improve the catalytic activity for oxygen reduction reaction. Journal of Power Sources, 2014, 251, 363-369.	7.8	54
32	N-doped porous transition metal-based carbon nanosheet networks as a multifunctional electrocatalyst for rechargeable zinc–air batteries. Chemical Communications, 2019, 55, 2924-2927.	4.1	54
33	Synergistic relationship between the three-dimensional nanostructure and electrochemical performance in biocarbon supercapacitor electrode materials. Sustainable Energy and Fuels, 2018, 2, 772-785.	4.9	53
34	High-performance all-solid-state asymmetric supercapacitors based on sponge-like NiS/Ni3S2 hybrid nanosheets. Materials Today Energy, 2019, 11, 211-217.	4.7	53
35	Soybean-derived mesoporous carbon as an effective catalyst support for electrooxidation of methanol. Journal of Power Sources, 2014, 248, 427-433.	7.8	52
36	Ultrathin willow-like CuO nanoflakes as an efficient catalyst for electro-oxidation of hydrazine. Journal of Power Sources, 2015, 289, 22-25.	7.8	52

#	Article	IF	CITATIONS
37	Highly dispersed ultrafine Pt nanoparticles on hydrophilic N-doped carbon tubes for improved methanol oxidation. RSC Advances, 2013, 3, 16949.	3.6	50
38	Synthesis of porous nitrogen and sulfur co-doped carbon beehive in a high-melting-point molten salt medium for improved catalytic activity toward oxygen reduction reaction. International Journal of Hydrogen Energy, 2018, 43, 5124-5132.	7.1	50
39	Hydrophobic 3D Fe/N/S doped graphene network as oxygen electrocatalyst to achieve unique performance of zinc-air battery. Chemical Engineering Journal, 2018, 353, 472-480.	12.7	50
40	Multidimensional regulation of Ni3S2@Co(OH)2 catalyst with high performance for wind energy electrolytic water. Journal of Power Sources, 2020, 446, 227348.	7.8	50
41	Highly Efficient and Stable Catalyst Based on Co(OH) <sub>2</sub> @Ni Electroplated on Cu-Metallized Cotton Textile for Water Splitting. ACS Applied Materials & Interfaces, 2019, 11, 29791-29798.	8.0	49
42	A High Faraday Efficiency NiMoO <sub>4</sub> Nanosheet Array Catalyst by Adjusting the Hydrophilicity for Overall Water Splitting. Chemistry - A European Journal, 2020, 26, 12067-12074.	3.3	49
43	Gas–liquid interface-mediated room-temperature synthesis of "clean―PdNiP alloy nanoparticle networks with high catalytic activity for ethanol oxidation. Chemical Communications, 2014, 50, 12877-12879.	4.1	48
44	Nano-engineered intrapores in nanoparticles of PtNi networks for increased oxygen reduction reaction activity. Journal of Power Sources, 2018, 374, 48-54.	7.8	48
45	PtSn/C catalysts for ethanol oxidation: The effect of stabilizers on the morphology and particle distribution. Journal of Power Sources, 2014, 247, 142-150.	7.8	47
46	Toward high practical capacitance of Ni(OH) <sub>2</sub> using highly conductive CoB nanochain supports. Journal of Materials Chemistry A, 2017, 5, 92-96.	10.3	45
47	CNx-modified Fe3O4 as Pt nanoparticle support for the oxygen reduction reaction. Journal of Solid State Electrochemistry, 2013, 17, 1021-1028.	2.5	43
48	Mesoporous CoS/Nâ€doped Carbon as HER and ORR Bifunctional Electrocatalyst for Water Electrolyzers and Zincâ€Air Batteries. ChemCatChem, 2019, 11, 1026-1032.	3.7	43
49	Design and synthesis of tremella-like Ni–Co–S flakes on co-coated cotton textile as high-performance electrode for flexible supercapacitor. Journal of Alloys and Compounds, 2020, 814, 151789.	5.5	43
50	Cu0.6Ni0.4Co2O4 nanowires, a novel noble-metal-free catalyst with ultrahigh catalytic activity towards the hydrolysis of ammonia borane for hydrogen production. International Journal of Hydrogen Energy, 2018, 43, 5541-5550.	7.1	41
51	Highly active porous Co–B nanoalloy synthesized on liquid-gas interface for hydrolysis of sodium borohydride. International Journal of Hydrogen Energy, 2018, 43, 17543-17555.	7.1	41
52	Synthesis of nitrogen-doped MnO/carbon network as an advanced catalyst for direct hydrazine fuel cells. Journal of Power Sources, 2019, 413, 209-215.	7.8	41
53	Chicken bone-derived N-doped porous carbon materials as an oxygen reduction electrocatalyst. Electrochimica Acta, 2014, 147, 520-526.	5.2	40
54	Fe(III) –Induced N Enrichment in the Surface of Carbon Materials Derived from Silk Fibroins and Its Effect on Electrocatalytic Oxygen Reduction. Journal of the Electrochemical Society, 2014, 161, F795-F802.	2.9	40

#	Article	IF	CITATIONS
55	Hollow-structured NiCoP nanorods as high-performance electrodes for asymmetric supercapacitors. Materials and Design, 2020, 193, 108807.	7.0	40
56	Charge state manipulation induced through cation intercalation into MnO2 sheet arrays for efficient water splitting. Chemical Engineering Journal, 2021, 417, 127894.	12.7	40
57	Highly efficient non-enzymatic glucose sensor based on CuxS hollow nanospheres. Applied Surface Science, 2019, 492, 407-416.	6.1	38
58	Mesoporous cobalt selenide/nitrogen-doped carbon hybrid as bifunctional electrocatalyst for hydrogen evolution and oxygen reduction reactions. Journal of Power Sources, 2019, 423, 1-8.	7.8	38
59	A highly efficient water electrolyser cell assembled by asymmetric array electrodes based on Co, Fe-doped Ni(OH)2 nanosheets. Applied Surface Science, 2020, 528, 146972.	6.1	38
60	Activating Cu/Fe2O3 nanoislands rooted on N-rich porous carbon nanosheets via the Mott-Schottky effect for rechargeable Zn-air battery. Chemical Engineering Journal, 2022, 442, 136128.	12.7	38
61	Amorphous PtNiP particle networks of different particle sizes for the electro-oxidation of hydrazine. RSC Advances, 2015, 5, 68655-68661.	3.6	37
62	Amorphous CoSn alloys decorated by Pt as high efficiency electrocatalysts for ethanol oxidation. Journal of Power Sources, 2011, 196, 8000-8003.	7.8	36
63	Tailoring nanopores within nanoparticles of PtCo networks as catalysts for methanol oxidation reaction. Electrochimica Acta, 2017, 255, 55-62.	5.2	36
64	Highly conductive copolymer/sulfur composites with covalently grafted polyaniline for stable and durable lithium-sulfur batteries. Electrochimica Acta, 2019, 321, 134678.	5.2	36
65	How to get to best oxygen evolution behavior from the electrolysis practice of the seawater. International Journal of Hydrogen Energy, 2021, 46, 12936-12943.	7.1	35
66	Integrating Ni nanoparticles into MoN nanosheets form Schottky heterojunctions to boost its electrochemical performance for water electrolysis. Journal of Alloys and Compounds, 2021, 867, 158983.	5.5	35
67	An advantageous method for methanol oxidation: Design and fabrication of a nanoporous PtRuNi trimetallic electrocatalyst. Journal of Power Sources, 2011, 196, 9346-9351.	7.8	34
68	Selenium-Functionalized Carbon as a Support for Platinum Nanoparticles with Improved Electrochemical Properties for the Oxygen Reduction Reaction and CO Tolerance. Journal of the Electrochemical Society, 2013, 160, H266-H270.	2.9	34
69	Synthesis of carbon-supported PdSn–SnO2 nanoparticles with different degrees of interfacial contact and enhanced catalytic activities for formic acid oxidation. Physical Chemistry Chemical Physics, 2013, 15, 13999.	2.8	33
70	N-doped porous carbon material made from fish-bones and its highly electrocatalytic performance in the oxygen reduction reaction. RSC Advances, 2015, 5, 48965-48970.	3.6	33
71	Solid-state-reaction synthesis of cotton-like CoB alloy at room temperature as a catalyst for hydrogen generation. Journal of Colloid and Interface Science, 2016, 475, 149-153.	9.4	33
72	Manganese dioxide core–shell nanostructure to achieve excellent cycling stability for asymmetric supercapacitor applications. RSC Advances, 2017, 7, 33635-33641.	3.6	33

#	Article	IF	CITATIONS
73	A 3D petal-like Ni <sub>3</sub> S <sub>2</sub> /CoNi <sub>2</sub> S <sub>4</sub> hybrid grown on Ni foam as a binder-free electrode for energy storage. Sustainable Energy and Fuels, 2018, 2, 1791-1798.	4.9	33
74	Implanting Cobalt Atom Clusters within Nitrogenâ€Doped Carbon Network as Highly Stable Cathode for Lithium–Sulfur Batteries. Small Methods, 2021, 5, e2100066.	8.6	33
75	N-Doped Carbon Networks Containing Inserted FeN <sub><i>x</i></sub> @NC Nanospheroids and Bridged by Carbon Nanotubes as Enhanced Catalysts for the Oxygen Reduction Reaction. ACS Sustainable Chemistry and Engineering, 2020, 8, 6979-6989.	6.7	32
76	Ultrafine amorphous PtNiP nanoparticles supported on carbon asÂefficiency electrocatalyst for oxygen reduction reaction. Journal of Power Sources, 2014, 259, 87-91.	7.8	31
77	Control of CuO nanocrystal morphology from ultrathin "willow-leaf―to "flower-shaped―for increased hydrazine oxidation activity. Journal of Power Sources, 2015, 300, 344-350.	7.8	31
78	Inserting ultrafine NiO nanoparticles into amorphous NiP sheets by <i>in situ</i> phase reconstruction for high-stability of the HER catalysts. Nanoscale, 2021, 13, 13703-13708.	5.6	31
79	Pt decorating of PdNi/C as electrocatalysts for oxygen reduction. Electrochimica Acta, 2010, 55, 1519-1522.	5.2	30
80	Hierarchical core-shell structured CoNi2S4/Ni3S2@Ni(OH)2 nanosheet arrays as electrode for electrochemical energy storage. Journal of Alloys and Compounds, 2019, 785, 684-691.	5.5	30
81	Ultrastable NiFeOOH/NiFe/Ni electrocatalysts prepared by in-situ electro-oxidation for oxygen evolution reaction at large current density. Applied Surface Science, 2021, 564, 150440.	6.1	30
82	Effect of stabilizers on the synthesis of palladium–nickel nanoparticles supported on carbon for ethanol oxidation in alkaline medium. Journal of Power Sources, 2014, 260, 12-18.	7.8	29
83	Three-dimensional iron, nitrogen-doped carbon foams as efficient electrocatalysts for oxygen reduction reaction in alkaline solution. Electrochimica Acta, 2014, 142, 317-323.	5.2	29
84	MnO/Nâ€Doped Mesoporous Carbon as Advanced Oxygen Reduction Reaction Electrocatalyst for Zinc–Air Batteries. Chemistry - A European Journal, 2019, 25, 2868-2876.	3.3	29
85	Hydrophilic Ni(OH)2@CoB nano-chains with shell-core structure as an efficient catalyst for oxygen evolution reaction. Journal of Alloys and Compounds, 2020, 844, 156129.	5.5	29
86	Evolution of the electrocatalytic activity of carbon-supported amorphous platinum–ruthenium–nickel–phosphorous nanoparticles for methanol oxidation. Journal of Power Sources, 2014, 268, 498-507.	7.8	28
87	Cow dung-derived nitrogen-doped carbon as a cost effective, high activity, oxygen reduction electrocatalyst. RSC Advances, 2015, 5, 27112-27119.	3.6	28
88	Enhanced Cycleability of Amorphous MnO2 by Covering on α-MnO2 Needles in an Electrochemical Capacitor. Materials, 2017, 10, 988.	2.9	28
89	Electrocatalyst based on Ni2P nanoparticles and NiCoP nanosheets for efficient hydrogen evolution from urea wastewater. Journal of Colloid and Interface Science, 2022, 608, 2932-2941.	9.4	28
90	SnO2-embedded worm-like carbon nanofibers supported Pt nanoparticles for oxygen reduction reaction. Electrochimica Acta, 2014, 141, 13-19.	5.2	27

#	Article	IF	CITATIONS
91	Room-temperature synthesis with inert bubble templates to produce "clean―PdCoP alloy nanoparticle networks for enhanced hydrazine electro-oxidation. RSC Advances, 2015, 5, 9837-9842.	3.6	27
92	A Co-N-doped carbonized egg white as a high-performance, non-precious metal, electrocatalyst for oxygen reduction. Journal of Solid State Electrochemistry, 2015, 19, 1727-1733.	2.5	27
93	Achieving highly practical capacitance of MnO <sub>2</sub> by using chain-like CoB alloy as support. Nanoscale, 2018, 10, 7813-7820.	5.6	27
94	Conductive Sulfur-Rich Copolymer Composites as Lithium–Sulfur Battery Electrodes with Fast Kinetics and a High Cycle Stability. ACS Sustainable Chemistry and Engineering, 2020, 8, 10389-10401.	6.7	27
95	Porous hetero-structured nickel oxide/nickel phosphide nanosheets as bifunctional electrocatalyst for hydrogen production via urea electrolysis. Journal of Colloid and Interface Science, 2022, 615, 163-172.	9.4	27
96	Carbon-supported platinum-decorated nickel nanoparticles for enhanced methanol oxidation in acid media. Journal of Solid State Electrochemistry, 2012, 16, 1049-1054.	2.5	26
97	Synthesis of ultrafine amorphous PtP nanoparticles and the effect of PtP crystallinity on methanol oxidation. RSC Advances, 2014, 4, 20722-20728.	3.6	26
98	Mesoporous nitrogen-doped carbon derived from carp with high electrocatalytic performance for oxygen reduction reaction. Journal of Power Sources, 2015, 278, 213-217.	7.8	26
99	The effect of the internal magnetism of ferromagnetic catalysts on their catalytic activity toward oxygen reduction reaction under an external magnetic field. Ionics, 2016, 22, 2195-2202.	2.4	26
100	Harvesting a 3D N-Doped Carbon Network from Waste Bean Dregs by Ionothermal Carbonization as an Electrocatalyst for an Oxygen Reduction Reaction. Materials, 2017, 10, 1366.	2.9	26
101	The Effect of PtRulr Nanoparticle Crystallinity in Electrocatalytic Methanol Oxidation. Materials, 2013, 6, 1621-1631.	2.9	25
102	A Volcano Curve: Optimizing Activity of Shell-Core PtxRuy@PdCu/C Catalysts for Methanol Oxidation by Tuning Pt/Ru Ratio. Journal of the Electrochemical Society, 2013, 160, H219-H223.	2.9	25
103	Moltenâ€ <del>S</del> alt Media Synthesis of Nâ€Doped Carbon Tubes Containing Encapsulated Co Nanoparticles as a Bifunctional Air Cathode for Zincâ€Air Batteries. Chemistry - A European Journal, 2020, 26, 10752-10758.	3.3	25
104	Nanoporous PdNi/C Electrocatalyst Prepared by Dealloying Highâ€Ni ontent PdNi Alloy for Formic Acid Oxidation. Fuel Cells, 2012, 12, 1129-1133.	2.4	24
105	Hierarchical core–shell structured Ni <sub>3</sub> S <sub>2</sub> /NiMoO <sub>4</sub> nanowires: a high-performance and reusable electrochemical sensor for glucose detection. Analyst, The, 2019, 144, 4925-4934.	3.5	24
106	Hollow core-shell structured Cu2O@Cu1.8S spheres as novel electrode for enzyme free glucose sensing. Materials Science and Engineering C, 2019, 95, 174-182.	7.3	22
107	Fe3C-inserted "tube plugging into porous network―nanohybrids as advanced sulfur hosts for lithium-sulfur batteries. Journal of Alloys and Compounds, 2021, 877, 160286.	5.5	22
108	Three-dimensional N-doped super-hydrophilic carbon electrodes with porosity tailored by Cu <sub>2</sub> O template-assisted electrochemical oxidation to improve the performance of electrical double-layer capacitors. Journal of Materials Chemistry A, 2021, 9, 2928-2936.	10.3	21

#	Article	IF	CITATIONS
109	Egg White Derived Tremella-Like Mesoporous Carbon as Efficient Non-Precious Electrocatalyst for Oxygen Reduction. Journal of the Electrochemical Society, 2014, 161, H637-H642.	2.9	20
110	Cobalt-nickel phosphides@carbon spheres as highly efficient and stable electrocatalyst for hydrogen evolution reaction. Catalysis Communications, 2019, 124, 1-5.	3.3	20
111	Uniform Bamboo-like N-Doped Carbon Nanotubes Derived from a g-C <sub>3</sub> N <sub>4</sub> Substrate Grown via Anchoring Effect to Boost the Performance of Metal–Air Batteries. ACS Applied Energy Materials, 2020, 3, 11213-11222.	5.1	20
112	Ni2P nanoparticles-inserted NiFeP nanosheets with rich interfaces as efficient catalysts for the oxygen evolution reaction. Journal of Alloys and Compounds, 2022, 903, 163855.	5.5	20
113	Ultra-high surface area and mesoporous N-doped carbon derived from sheep bones with high electrocatalytic performance toward the oxygen reduction reaction. Journal of Solid State Electrochemistry, 2017, 21, 2947-2954.	2.5	19
114	Mn Nanoparticles Encapsulated within Mesoporous Helical Nâ€Đoped Carbon Nanotubes as Highly Active Air Cathode for Zinc–Air Batteries. Advanced Sustainable Systems, 2019, 3, 1900085.	5.3	19
115	An effective electrocatalyst for ethanol oxidation: Pt-modified IrCu alloy nanoparticle. Ionics, 2011, 17, 595-601.	2.4	18
116	Effect of Ni Core Structure on the Electrocatalytic Activity of Pt-Ni/C in Methanol Oxidation. Materials, 2013, 6, 2689-2700.	2.9	18
117	Lysine-derived mesoporous carbon nanotubes as a proficient non-precious catalyst for oxygen reduction reaction. Journal of Power Sources, 2014, 269, 54-60.	7.8	18
118	Porous-sheet-assembled Ni(OH) <sub>2</sub> /NiS arrays with vertical in-plane edge structure for supercapacitors with high stability. Dalton Transactions, 2019, 48, 17364-17370.	3.3	18
119	Mo-doped Cu0.5Ni0.5Co2O4 nanowires, a strong substitute for noble-metal-based catalysts towards the hydrolysis of ammonia borane for hydrogen production. Catalysis Communications, 2018, 114, 89-92.	3.3	18
120	Nitrogen-doped carbon coated palygorskite as an efficient electrocatalyst support for oxygen reduction reaction. Electrochimica Acta, 2011, 56, 4526-4531.	5.2	17
121	Nanoparticulate TiO2-promoted PtRu/C catalyst for methanol oxidation. Ionics, 2013, 19, 529-534.	2.4	16
122	Grain boundaries of Co(OH)2-Ni-Cu nanosheets on the cotton fabric substrate for stable and efficient electro-oxidation of hydrazine. International Journal of Hydrogen Energy, 2019, 44, 24591-24603.	7.1	16
123	Manganese-Assisted Annealing Produces Abundant Macropores in a Carbon Aerogel to Enhance Its Oxygen Reduction Catalytic Activity in Zinc–Air Batteries. ACS Sustainable Chemistry and Engineering, 2021, 9, 5526-5535.	6.7	16
124	Facile synthesis of core–shell FeOOH@MnO2 nanomaterials with excellent cycling stability for supercapacitor electrodes. Journal of Materials Science: Materials in Electronics, 2017, 28, 6481-6487.	2.2	15
125	Synthesis of high surface area mesoporous MnO 2 via a "metastable―aqueous interfacial reaction. Journal of Colloid and Interface Science, 2017, 503, 76-85.	9.4	15
126	MOF derived graphitic carbon nitride/oxygen vacancies-rich zinc oxide nanocomposites with enhanced supercapacitive performance. Ionics, 2020, 26, 5155-5165.	2.4	15

#	Article	IF	CITATIONS
127	Nanostructured Pt supported on cocoon-derived carbon as an efficient electrocatalyst for methanol oxidation. Journal of Solid State Electrochemistry, 2014, 18, 1503-1512.	2.5	14
128	Integration of supercapacitors into printed circuit boards. Journal of Energy Storage, 2018, 19, 28-34.	8.1	14
129	Layer-structured FeCo bihydroxide as an ultra-stable bifunctional electrocatalyst for water splitting at high current densities. Sustainable Energy and Fuels, 2021, 5, 2747-2752.	4.9	13
130	1D NiHPO4 nanotubes prepared using dissolution equilibrium as bifunctional electrocatalyst for high-efficiency water splitting. Journal of Power Sources, 2021, 513, 230543.	7.8	13
131	Synergistic Effect between Monodisperse Fe <sub>3</sub> O <sub>4</sub> Nanoparticles and Nitrogen-Doped Carbon Nanosheets to Promote Polysulfide Conversion in Lithium–Sulfur Batteries. ACS Applied Materials & Interfaces, 2022, 14, 16310-16319.	8.0	13
132	Salt stress-induced expression of rice AOX1a is mediated through an accumulation of hydrogen peroxide. Biologia (Poland), 2010, 65, 868-873.	1.5	12
133	Performance evaluation of functionalized carbon aerogel as oxygen reduction reaction electrocatalyst in zinc-air cell. Journal of Power Sources, 2021, 511, 230458.	7.8	12
134	FeCo nanoclusters inserted N,S –doped carbon foams as bifunctional electrocatalyst for high-performance rechargeable Zn-air batteries. Journal of Power Sources, 2022, 538, 231592.	7.8	12
135	Tailoring the porous structure of N-doped carbon for increased oxygen reduction reaction activity. Catalysis Communications, 2018, 107, 29-32.	3.3	11
136	Tuning the extent of porosity and composition of N-doped carbon materials by NaNO3 and its effect on electrochemical activity. Materials Research Bulletin, 2018, 104, 134-142.	5.2	11
137	Dual-shelled Cu2O@Cu9S5@MnO2 hollow spheres as advanced cathode material for energy storage. Journal of Alloys and Compounds, 2019, 805, 977-983.	5.5	11
138	Toward high performance of zinc-air battery using hydrophobic carbon foam-based diffusion electrode. Journal of Industrial and Engineering Chemistry, 2019, 71, 284-292.	5.8	11
139	Tailoring hollow structure within NiCoP nanowire arrays via nanoscale Kirkendall diffusion to enhance hydrogen evolution reaction. Nanotechnology, 2020, 31, 425404.	2.6	11
140	V2O5-SiO2 hybrid as anode material for aqueous rechargeable lithium batteries. Ionics, 2016, 22, 1593-1601.	2.4	10
141	A Highly Crosslinked and Conductive Sulfur-Rich Copolymer with Grafted Polyaniline for Stable Cycling Lithium–Sulfur Batteries. Journal of the Electrochemical Society, 2020, 167, 020530.	2.9	10
142	Roughening the surface of porous NiCoP rod-like arrays <i>via</i> the <i>in situ</i> growth of NiCoP <sub>4</sub> O <sub>12</sub> nanoislands enables highly efficient energy storage. Dalton Transactions, 2022, 51, 4484-4490.	3.3	10
143	Using sp2 N atom anchoring effect to prepare ultrafine vanadium nitride particles on porous nitrogen-doped carbon as cathode for lithium-sulfur battery. Journal of Colloid and Interface Science, 2022, 623, 306-317.	9.4	10
144	Nano-sized Co/Co(OH)2 core-shell structure synthesized in molten salt as electrode materials for supercapacitors. Ionics, 2017, 23, 725-730.	2.4	9

#	Article	IF	CITATIONS
145	An industry-applicable hybrid electrode for large current density hydrogen evolution reaction. Journal of Power Sources, 2021, 516, 230635.	7.8	9
146	A post-synthesis surface reconstructed carbon aerogel as an enhanced oxygen reduction reaction cation catalyst for zinc–air batteries. Catalysis Science and Technology, 2020, 10, 5288-5297.	4.1	8
147	In-site hydrogen bubble template method to prepare Ni coated metal meshes as effective bi-functional electrodes for water splitting. Dalton Transactions, 2022, 51, 9681-9688.	3.3	8
148	Nano-engineering PdNi networks by voltammetric dealloying for ethanol oxidation. Journal of Applied Electrochemistry, 2019, 49, 39-44.	2.9	7
149	Sponge-like carbon containing nitrogen and iron provides a non-precious oxygen reduction catalyst. Journal of Solid State Electrochemistry, 2015, 19, 1181-1186.	2.5	6
150	Simplifying the creation of iron compound inserted, nitrogen-doped carbon nanotubes and its catalytic application. Journal of Alloys and Compounds, 2021, 857, 157543.	5.5	6
151	Copper mesh supported nickel nanowire array as a catalyst for the hydrogen evolution reaction in high current density water electrolysis. Dalton Transactions, 2022, 51, 5309-5314.	3.3	6
152	Effect of surface reconstruction induced by different electrochemical methods on hydrogen evolution performance of Ni2P array catalysts. International Journal of Hydrogen Energy, 2022, 47, 17097-17106.	7.1	6
153	Surfacial carbonized palygorskite as support for high-performance Pt-based electrocatalysts. Journal of Solid State Electrochemistry, 2013, 17, 2009-2015.	2.5	5
154	Flexible electrode with composite structure for large-scale production. Journal of Alloys and Compounds, 2019, 810, 151871.	5.5	5
155	Catalytically Active CoSe <sub>2</sub> Supported on Nitrogenâ€Doped Three Dimensional Porous Carbon as a Cathode for Highly Stable Lithiumâ€5ulfur Battery. ChemPhysChem, 2022, 23, .	2.1	5
156	Synthesis of hierarchical threeâ€dimensional CuO spindles for highly sensitive glucose determination. Micro and Nano Letters, 2016, 11, 870-875.	1.3	4
157	Engineering the densities of grain boundaries within particle-assembled NiCo2O4 rods by sulfurization for effective water electrolysis. Journal of Electroanalytical Chemistry, 2022, 908, 116098.	3.8	4
158	Ultra-dispersed copper nanoparticles constructing crystalline-amorphous interface sites for alkaline water splitting. Journal of Colloid and Interface Science, 2022, 627, 650-660.	9.4	4
159	Highly electrocatalytic three-dimensional chain-like nickel-based electrocatalysts with hierarchical structures for hydrogen evolution reactions. Dalton Transactions, 2021, 50, 14724-14729.	3.3	2
160	Chain-like SnO2-CNxNanocomposite Supported Pt Nanoparticles and Their Application in the Electrocatalytic Oxidation of Ethanol in Acid Medium. Journal of the Electrochemical Society, 2014, 161, H860-H866.	2.9	1